NASA TECHNICAL MEMORANDUM

NASA TM X-52656

NASA TM X-52656

N10K-00

CORRELATION OF CRITICAL HEAT FLUX FOR WETTING FLUIDS AND CHANNELS OF VARIOUS CROSS SECTIONS

by Uwe H. von Glahn
Lewis Research Center
Cleveland, Ohio

TECHNICAL PAPER proposed for presentation at
Fourth International Heat Transfer Conference
Versailles/Paris, France, August 31-September 5, 1970

CORRELATION OF CRITICAL HEAT FLUX FOR WETTING FLUIDS AND CHANNELS OF VARIOUS CROSS SECTIONS

by Uwe H. von Glahn

Lewis Research Center
Cleveland, Ohio

TECHNICAL PAPER proposed for presentation at

Fourth International Heat Transfer Conference
Versailles/Paris, France, August 31-September 5, 1970

NATIONAL AERONAUTICS AND SPACE ADMINISTRATION

CORRELATION OF CRITICAL HEAT FLUX FOR WETTING FLUIDS AND CHANNELS OF VARIOUS CROSS SECTIONS

Uwe H. von Glahn
NASA Lewis Research Center, Cleveland, Ohio

E-5232

Abstract

An empirical correlation for predicting critical boiling heat flux (burnout condition) under conditions of stable flow for wetting fluids is presented. The correlation includes data for water, nitrogen, hydrogen, and potassium. Flow passage geometries considered include circular tubes, annular tubes, and rectangular channels. The effect of swirl devices on critical heat flux is discussed and an acceleration correlation parameter is included. All fluid property terms are evaluated at the fluid saturation temperature associated with the burnout condition.

INTRODUCTION

In the design considerations of boiling fluid devices to be used for the generation of large amounts of vapor the best efficiency in terms of large heat fluxes and low wall-to-bulk temperature differences can be achieved within the nucleate boiling regime. Transition from the nucleate to the film boiling regime, with its accompanying high wall-to-bulk temperature differences and lower heat fluxes, will lower the vapor generation efficiency. The heat flux associated with the transition from nucleate to film boiling is herein called the critical heat flux. For a flowing system this critical heat flux can be defined as the flux immediately before the transition from a high heat transfer coefficient to a lower value at some unspecified location along the flow passage. The point along the flow passage surface at which this transition in heat transfer coefficient occurs is frequently called the burnout point because of the possibility of material failure. The distance measured along the flow passage axis from the inlet to the burnout location is designated as the critical length.

Critical heat flux values differing by over 100 percent can easily be obtained in a particular research system. These differences frequently can be attributed to: (1) the introduction of a compressible volume upstream of the heated test section [1], (2) dynamic coupling between the feed system and boiler tube [2], (3) techniques used in establishing a critical heat flux condition [3], or (4) gas content of the liquid [1]. These effects always produce low critical heat flux values. Since about 1958, however, many of the preceding effects have been recognized and minimized by researchers resulting in better burnout data and understanding of two-phase heat transfer problems.

In the present study, conducted at the NASA Lewis Research Center, a two-step correlation of critical boiling heat flux has been developed. The first step consists of the correlation of the critical heat flux in terms of a critical quality parameter for saturated conditions at the boiler inlet (H = 0). The second step is the correlation of the increased critical heat flux associated with conditions of subcooled liquid at the boiler inlet (H > 0). The fluid property parameters developed correlate fluids having such widely varying properties as hydrogen, nitrogen, potassium, and water.

BURNOUT CORRELATION WITH LIQUID (SUBCOOLING) ENTHALPY

A typical variation of critical heat flux with liquid (subcooling) enthalpy, H, for water is shown in Figure 1 for several flow rates at a fixed passage geometry and pressure level (circular tube, 1.08 cm diam; pressure, 6.9 MN/m^2). It can be seen that the slope of the q_c versus H curve increases with increasing values of flow rate. Also shown on the curves is the liquid enthalpy point at which the critical quality is zero; at greater values of H than that noted, subcooled (bulk) burnout occurs while at lower H-values burnout occurs with net vapor generation. A single curve can be drawn at each flow rate regardless of whether the critical heat flux is in the net vapor generation regime or in the subcooled regime [4].

The present study showed that the critical quality, X_o, at which burnout occurs can be related to a combination of several well-known heat transfer and hydrodynamic numbers and ratios of vapor-to-liquid fluid properties. In very general terms the correlation can be expressed as:

$$X_o = f(We,\ Re,\ Pr,\ B'_{O-N}, \mu_v/\mu_L, \Delta\rho/\rho_v, D_e/D_h, L/D_h, a_R) \tag{1}$$

The critical quality, X_o, when H = 0, is defined as:

$$X_o = Q_o/\lambda W = (4q_oL)/(GD_e\lambda) \tag{2}$$

A study [5] of the various nondimensional relations evolved a dimensionless fluid property parameter that, with additional ratios of density and viscosity provided a useful tool for correlation of experimental data. This dimensionless fluid property parameter consisted of:

$$N_B = \left(\mu_v{}^2\sqrt{g\,\Delta p}\right)\Big/\left[\rho_v(\sigma)^{1.5}\right] \tag{3}$$

and was arbitrarily designated as a boiling number in reference [5]. All fluid properties in equation (3) are evaluated at the saturation temperature associated with the burnout location. N_B consists of fluid property relations identical to those expressed by Reynolds number, Weber number, and the ratio of a characteristic dimension of the flow passage to a detachment bubble diameter, d, as follows:

$$N_B = \left[We_{D_h}/(Re_{D_h})^2\right](D_h/d) \tag{4}$$

The detachment bubble diameter in equation (4) is that size to which a bubble will grow before detaching from a surface with a fluid flow of zero velocity. In terms of the Bond-Newton number this bubble size is given by:

$$d = \left[B_{O-N}/f(\beta)\right]\sqrt{\sigma/g(\Delta\rho)} \tag{5}$$

Equation (5) was simplified for the wetting fluids considered herein by assuming that the bubble detachment angle, β, was sufficiently the same for all the fluids and did not vary with surface conditions of the flow passages. It was further assumed that the term $B_{O-N}/f(\beta)$ was a constant and equal to 1.0. Equation (5) then simplifies to:

$$d = \sqrt{\sigma / g(\Delta\rho)} \tag{6}$$

It was also assumed that the fluid velocity in the region of bubble formation was sufficiently low to be neglected as a significant factor in the correlation. Local velocity gradients could be included by the use of more complex equations and assumptions; for example, those of reference [6]. The ratio of D_h/d in equation (4) can now be written as:

$$D_h/d = \sqrt{g(\Delta\rho) D_h^2/\sigma} = B'_{O-N} \tag{7}$$

For the case of nonwetting fluids (mercury) or when wetting agents are used in a fluid, consideration of the bubble angle β must be included in the present correlation; however, this is beyond the scope of this paper.

Mass Velocity

As a first step, the relationship of the mass velocity to the critical heat flux was established. It was pointed out by Rohsenow [7] that a number of researchers have determined that the critical heat flux varies with about $\sqrt{G}$ at low flow rates and with about G at high flow rates. In evaluating the data ([3], [8], [9]) the present author concluded that an exponent e (approximately 0.5 to 1.0) for the mass velocity parameter can be related to the channel diameter, the detachment bubble size, and fluid properties. A simple equation that satisfies these criteria and provides a smooth transition for the exponent from 0.5 to 1.0 is given by:

$$e = 0.5\left\{1 + \frac{1}{1 + 0.2\left[\dfrac{100\,\rho_L\, d}{G\, Pr_v}\sqrt{\dfrac{g}{D_h}}\left(\dfrac{\mu_v}{\mu_L}\right)\right]^{5.0}}\right\} \tag{8}$$

In dimensionless parameters the critical quality then varies with mass velocity as follows:

$$X_o = f(Re_{d,v} Pr_v N_B)^e \tag{9}$$

Flow Passage Length-to-Size Ratio

Critical quality obtained with a circular tube [4] (tube diam, 1.08 cm; pressure, 6.9 MN/m^2) is shown in Figure 2 as a function of the mass velocity for several L/D_h ratios. This plot, on logarithmic scales, shows that the slopes of the curves vary with L/D_h ratio; at small values of L/D_h the slope is near -1.0 whereas at large values of L/D_h the slope approaches -0.5. The L/D_h relationship demonstrated by these curves can be expressed by:

$$(X_o)^a = \frac{f(Re_{d,v} Pr_v N_B)^e}{(L/D_h)^b} \tag{10}$$

where the exponent b is a complex variable of density ratio, N_B and L/D_h. The exponent b is given by:

$$b = 0.25\left\{1 + \frac{1}{1 + \left[\frac{1.6\times 10^{-10}}{N_B}\sqrt{\frac{\Delta\rho}{\rho_v}}\left(\frac{L}{D_h}\right)\right]^2}\right\} \qquad (11)$$

The exponent a for the critical quality will be discussed in the next section because it is also influenced by flow passage shape.

Flow Passage Shape

Critical quality is also influenced by the shape of the flow passage as determined from experiments in references [10], [11], and [12]. The effect of passage shape is accounted for by another variable in the previously noted exponent a in equation (10) as well as a multiplying factor for the right side of equation (10). This variable in both cases can be expressed by the ratio D_e/D_h. When used as a multiplier for the right side of equation (10) the ratio of D_e/D_h is raised to an exponent of 1.5.

The exponent for X_o in equation (10) is now written to include the effects of both L/D_h and D_e/D_h as follows:

$$a = \left[\frac{1}{1 + (B)(C)}\right] \qquad (12)$$

where

$$B = \frac{0.35\times 10^{-6}}{N_B}\left[\frac{1 + (0.0015\,\Delta\rho/\rho_v)^2}{1 + (0.00475\,L/D_h)^{2.25}}\right] \qquad (13)$$

and

$$C = \left(\frac{1}{1 + \left\{0.825\left[(D_e/D_h) - 1\right]\right\}^8}\right)^{0.125} \qquad (14)$$

Flow Passage Size

A dimensionless parameter, F_s, was obtained that related the ratio of the effective channel height, b_e, [13] to the detachment bubble diameter in order to account for the size trend shown by the data. F_s is given by:

$$F_s = \frac{1}{1 + 1.75(d/b_e)^{1.67}} \qquad (15)$$

and is used as a multiplier for the right side of equation (10).

For circular tubes and rectangular channels with parallel sides heated b_e was found to be 0.416D or one-half the channel height, respectively. For annular tubes with one diameter heated and rectangular channels with only one side heated b_e is the entire channel height above the heated surface.

Fluid Properties Parameter

In addition to the fluid properties included in the previously discussed parameters, a separate fluid properties term is necessary to correlate critical quality for different fluids and for the variation of critical quality with pressure level for a specific fluid. A parameter F_f provides the necessary correlation and is given by:

$$F_f = \frac{Pr_v^{1.5}}{(\mu_v/\mu_L)^{0.3}(N_B \times 10^6)^{0.85}} \tag{16}$$

The F_f parameter is also a multiplier term for the right side of equation (10).

Effect of Gravity and Flow Acceleration Devices

The effect of gravity on critical quality and critical heat flux has been explored both toward zero gravity as well as toward many gravities by numerous researchers. In general it has been found that for "real" gravity changes, the critical heat flux varies with the ratio $(g_x/g)^{0.25}$. When radial acceleration devices (such as twisted tapes, wire coils, etc.) are used to create an increased gravity field near the passage walls, large acceleration forces are required to provide significant changes in the value of the critical heat flux and critical quality. Conventional methods of calculating radial acceleration values for such devices as tapes and coils in tubes yields the following equation [14]:

$$a_R = \frac{2}{gD}\left(\frac{GX}{\rho_v K}\frac{\pi D}{P}\right)^{2.0} \tag{17}$$

The K in this equation is the ratio of the vapor-to-liquid velocity and is expressed as $\sqrt{\rho_L/\rho_v}$. Thus

$$a_R = \frac{2\pi^2}{g(\rho_L \rho_v)D}\left(\frac{XG}{P/D}\right)^2 = \frac{2\pi^2}{g(\rho_L \rho_v)D}\left(\frac{X_o G}{P/D}\right)^2 \tag{18}$$

These relationships do not account for slip between the vapor and the liquid, nor do they account for the condition of the liquid on the heated flow passage wall; i.e., whether the wall is fully wetted or rivulet flow is occurring. Consequently, if a_R is used in place of g_x the effect on critical quality will be greatly exaggerated. Water and potassium data (unpublished NASA data and [14], respectively) show that with typical radial acceleration devices g_x in terms of a_R can be expressed as:

$$g_x = \left[1 + (0.125\ a_R)^{0.667}\right]g \tag{19}$$

In the present correlation the effect of radial acceleration is given by:

$$F_g = (g/g_x)^{0.25} = \left[\frac{1}{1 + (0.125\ a_R)^{0.667}}\right]^{0.25} \tag{20}$$

The F_g-parameter is a multiplier for the right side of equation (10) and a function of the exponent e.

Complete Burnout Correlation for $H = 0$

The complete correlation for determining the critical quality and heat flux is summarized in the following relation:

$$(X_o)^a = f\left[\frac{(Re_{d,v}Pr_vN_BF_g)^e(D_e/D_h)^{1.5}(F_f)(F_s)}{(L/D_h)^b}\right] = f(Z) \tag{21}$$

Representative critical quality data for references [3], [4], [8], [9], [10], [11], and [12] are plotted in terms of equation (21) in the following Figures 3 to 5. It should be noted that the low-pressure water data and that for nitrogen, hydrogen, and potassium were all obtained at low flow rates so that the exponent e in equation (21) was generally near 0.5. The high-pressure water data, on the other hand, was obtained at large flow rates; consequently, the exponent e was effectively 1.0.

The range of D_e/D_h for the annular tubes and rectangular channels shown in Figure 4 was from 1.12 to 4.35. The physical size of the annular tubes varied from a combination of a heated $D_i = 0.95$ cm with an unheated $D_o = 1.8$ cm to a heated $D_i = 1.27$ cm with an unheated $D_o = 2.52$ cm. The rectangular channels had heated widths of 2.54 to 5.34 cm and unheated heights of 0.25 to 1.27 cm.

The solid curve shown in Figures 3 to 5 was obtained from a data fit using the relationships expressed by equation (21). The solid curve is expressed as:

$$(X_o)^a = \left[\frac{0.0035}{0.0035 + 0.1Z + (10Z)^4}\right]^{0.133} \tag{22}$$

from which

$$X_o = \left[\frac{0.0035}{0.0035 + 0.1Z + (10Z)^4}\right]^{0.133/a} \tag{23}$$

and

$$q_o = \left(\frac{GD_e\lambda}{4L}\right)\left[\frac{0.0035}{0.0035 + 0.1Z + (10Z)^4}\right]^{0.133/a} \tag{24}$$

CRITICAL HEAT FLUX WITH ENTERING LIQUID ENTHALPY

The critical heat flux for a fixed geometry and pressure level increases with increasing subcooling (liquid) enthalpy for a given fluid (Fig. 1). The increase in critical heat flux over that given by equation (24) depends on the initial value of the critical heat flux when $H = 0$ and the associated flow rate, L/D_h ratio and latent heat; i.e., critical quality functions. The present study has assumed that the total critical heat flux with liquid subcooling at the boiler entrance can be obtained from the superposition of q_o and a Δq that accounts for the effects of the liquid subcooling. Thus

$$q_c = q_o + \Delta q \tag{25}$$

Experimental data from reference [4] were used to determine the necessary relationships for Δq. A good representation of these data can be obtained from the following equation:

$$\Delta q = \frac{15500\left(\dfrac{\Delta\rho}{\rho_v}\right)^{0.6}\left(\dfrac{\mu_v}{\mu_L}\right)^{1.67}\left(\dfrac{\sigma^2}{g\mu_v^2 D_h}\right)^{0.33}\sqrt{1 - X_o}\,(H/\lambda)^{\sqrt{2-X_o}}\left[1 + 8.5(1 - X_o)^{10}\right]}{1 + (0.002\ X_o\ L/D_h)^2(\rho_v/\Delta\rho)^{0.33}(\mu_L/\mu_v)} \tag{26}$$

The value of X_o in equation (26) is obtained by use of equation (23). Comparisons of the measured Δq for representative flow conditions and circular tubes are shown in Figure 6 as a function of subcooling (liquid) enthalpy. Similar comparisons for a representative annular tube ($D_o/D_i = 1.8$ cm/0.95 cm) and a rectangular channel (0.64×5.33 cm) are shown in Figure 7. While the data shown in Figures 6 and 7 are all for a pressure of 6.9 MN/m^2, similar results were obtained over a range of pressures from 3.85 to 13.8 MN/m^2.

CONCLUDING REMARKS

From an analysis of critical heat flux data obtained with water, nitrogen, hydrogen, and potassium, empirical equations have been evolved that correlate critical quality and critical heat flux over a wide range of operating conditions and flow passage sizes and shapes. Correlation was achieved by using established dimensionless groupings and fluid property ratios (vapor to liquid) known to influence boiling. All fluid properties are evaluated at the saturation temperature associated with the burnout location. The correlation is suitable for both net vapor generation conditions as well as bulk (subcooled) burnout conditions. The inclusion of an acceleration term should be useful in predicting the improvement in boiler burnout by the application of internal flow swirl devices.

On the basis of a preliminary study, the author believes that critical heat flux values for more complex geometries, such as rod bundles, may be estimated by use of the present correlation. Such estimates require the selection of suitable shape and size factors. For example, a single rod inside a rod bundle can perhaps be analyzed by considering the flow passage periphery to be represented locally by an annulus or channel heated from both sides. A rod on the outside of the bundle adjacent to the shell can be considered similarly but with only one surface heated.

NOMENCLATURE

a_R	radial acceleration
b_e	effective channel height
B_{O-N}	Bond Newton number
B'_{O-N}	modified Bond-Newton number
D	flow passage diameter
d	detachment bubble diameter
D_h	hydraulic diameter (based on wetted perimeter)
D_e	equivalent diameter (based on heated perimeter)
G	mass velocity
g	acceleration at standard earth gravity
g_x	acceleration at other than standard earth gravity
H	liquid (subcooling) enthalpy measured from saturation
L	channel length to burnout
N_B	boiling number
P	boiler insert pitch
Pr	Prandtl number
Q_c	rate of critical heat transfer
q_c	total critical heat flux, $q_o + \Delta q$
q_o	critical heat flux with saturated fluid at boiler inlet
Δq	increase in critical heat flux above q_o when fluid at boiler inlet is subcooled $(H > 0)$
Re	Reynolds number
W	mass flow rate
We	Weber number
X	thermodynamic quality
X_o	critical quality with saturated fluid at boiler inlet $(H = 0)$

Greek Symbols

β	bubble contact angle
λ	latent heat
μ	dynamic viscosity
ρ	density
$\Delta\rho$	density difference between liquid and vapor
σ	vapor-liquid surface tension

Subscripts

d	bubble diameter
D_h	hydraulic diameter
i, o	inside and outside diameters of annular tube, respectively
L	liquid
v	vapor

REFERENCES

[1] W. H. Lowdermilk, et al.: Investigation of boiling burnout and flow stability for water flowing in tubes. NACA TN 4382 (1958).

[2] R. G. Dorsch: Frequency response of a forced-flow single-tube boiler. Symposium on Two Phase Flow Dynamics, Technical University of Eindhoven and EURATOM, Eindhoven, The Netherlands (Sept. 4-9, 1967).

[3] J. P. Lewis, et al.: Boiling heat transfer to liquid hydrogen and nitrogen in forced flow. NASA TN D-1314 (1962).

[4] B. Thompson and R. V. MacBeth: Boiling water heat transfer burnout in uniformly heated round tubes: a compilation of world data with accurate correlations. AEEW-R-356 (1964).

[5] U. H. von Glahn: An empirical correlation of critical boiling heat flux in forced flow upward through uniformly heated tubes. NASA TN D-1285 (1962).

[6] I. G. Druker: Critical heat flux with steam-water mixture flowing in tubes. Teploenergetrka, vol. 14, no. 4, p. 76/78 (1967).

[7] W. M. Rohsenow: Developments in heat transfer. The MIT Press, Cambridge, Mass. (1964).

[8] G. F. Hewitt, et al.: Burnout and film flow in the evaporation of water in tubes. AERE- R 4864 (1965).

[9] H. W. Hoffman: Recent experimental results in ORNL studies with boiling potassium. Proceedings of 1963 High-Temperature Liquid-Metal Heat Transfer Technology Meeting. ORNL-3605, vol. 1, p. 334/350, Oak Ridge National Lab. (Nov. 1964).

[10] F. E. Tippets: Critical heat flux and flow pattern characteristics of high pressure boiling water in forced convection. GEAP-3766, General Electric Co., (Apr. 1962).

[11] S. Levy: Prediction of the critical heat flux in forced convection flow. GEAP-3961, General Electric Co. (June 1962).

[12] R. A. DeBortoli, et al.: Forced-convection heat transfer burnout studies for water in rectangular channels and round tubes at pressures above 500 psia. WAPD-188, Westinghouse Electric Corp. (Oct. 1958).

[13] U. H. von Glahn: On the empirical correlation of critical boiling heat flux for channels of various cross sections and orientation. NASA TN D-1656 (1963).

[14] J. R. Peterson: High-performance "once-through" boiling of potassium in single tubes at saturation temperatures of 1500^{o} to 1750^{o} F. NASA CR-842 (1967).

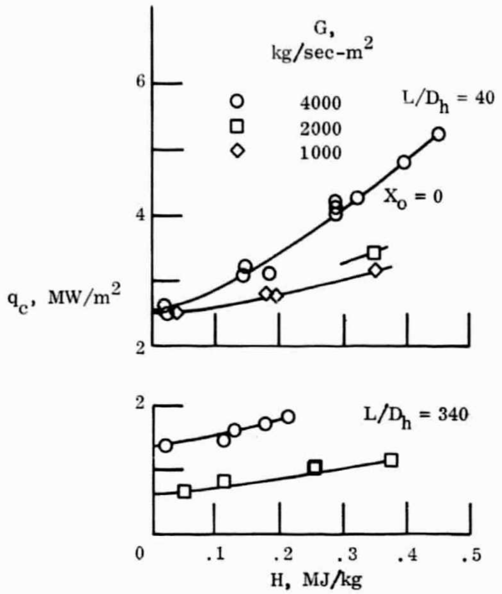

Figure 1. - Typical variation of critical heat flux with liquid (subcooled) enthalpy [4].

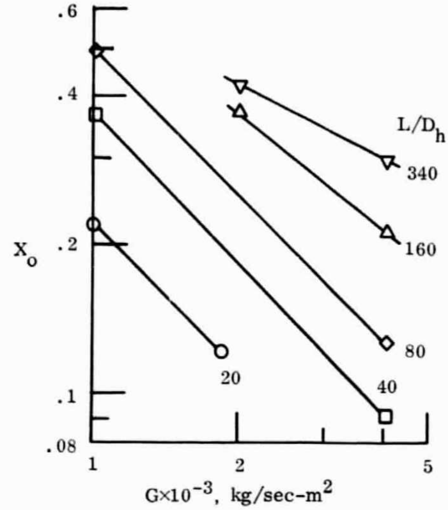

Figure 2. - Typical variation of critical quality with mass velocity (H = 0), [4].

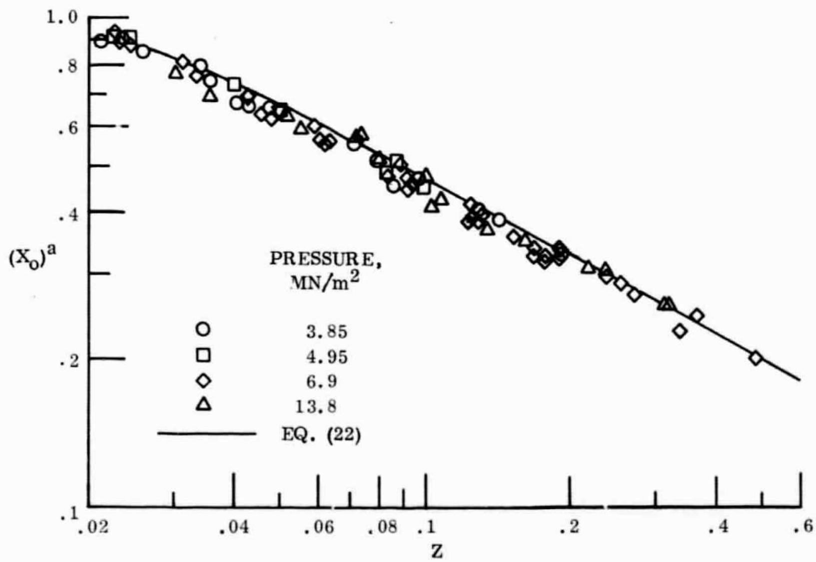

Figure 3. - Correlation of critical quality for water in circular tubes at high pressures, [4].

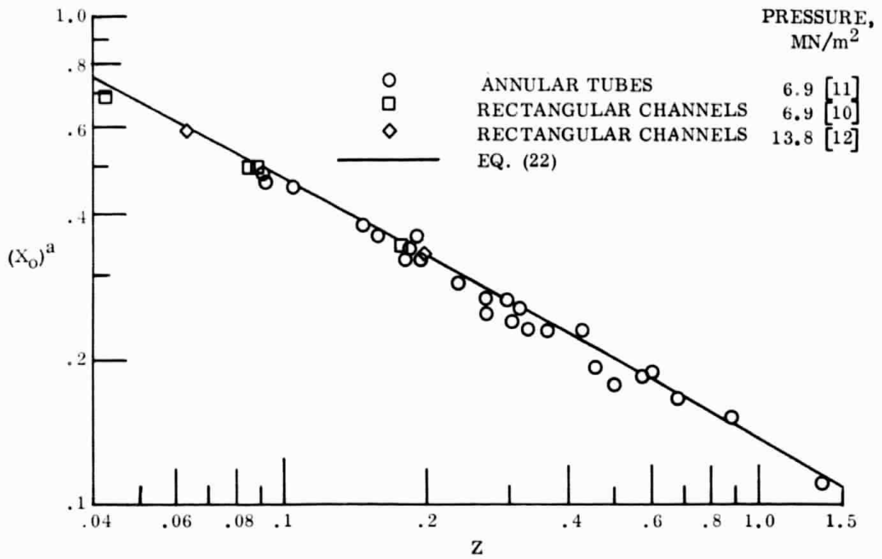

Figure 4. - Correlation of critical quality for channels of various cross sections.

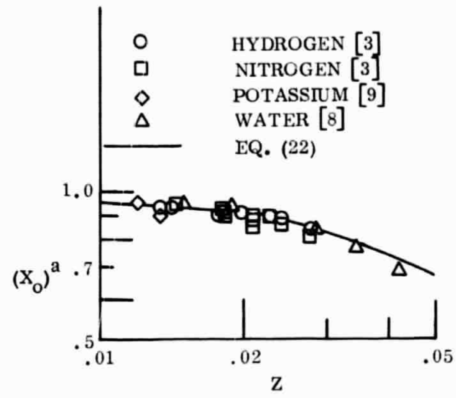

Figure 5. - Correlation of critical quality in circular tubes for various fluids. Pressure, <0.35 MN/m^2.

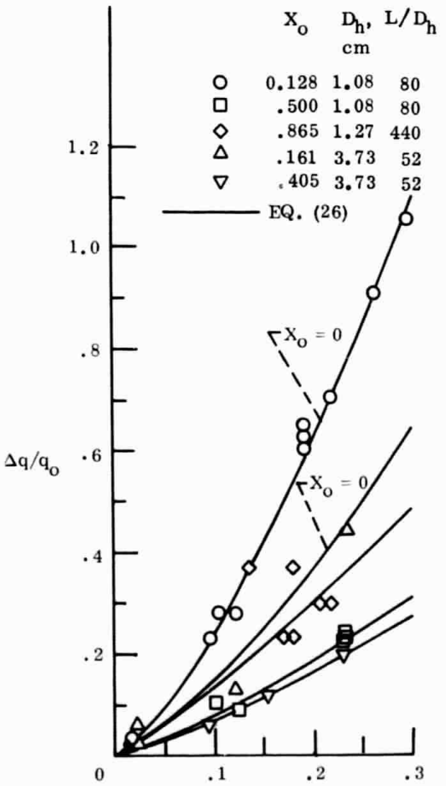

Figure 6. - Correlation of liquid enthalpy effect on critical heat flux. Circular tubes; pressure, 6.9 MN/m^2, [4].

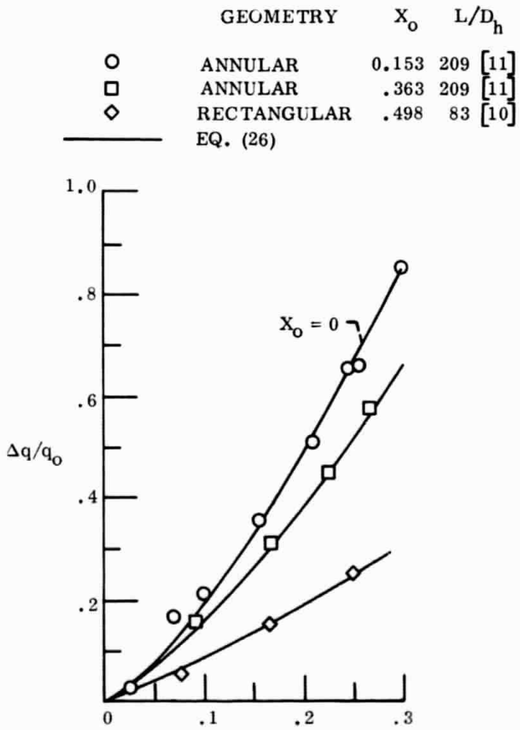

Figure 7. - Correlation of liquid enthalpy effect on critical heat flux. Various shaped channels; pressure, 6.9 MN/m^2.

NASA-CLEVELAND, OHIO E-5232